ANNUAL REPORT 2010

UIUC, August 12, 2010

Modeling Heat Transfer, Precipitate Formation and Grain Growth in Casting and Reheating

Kun Xu
(Ph.D. Student)

Department of Mechanical Science and Engineering
University of Illinois at Urbana-Champaign

Objective

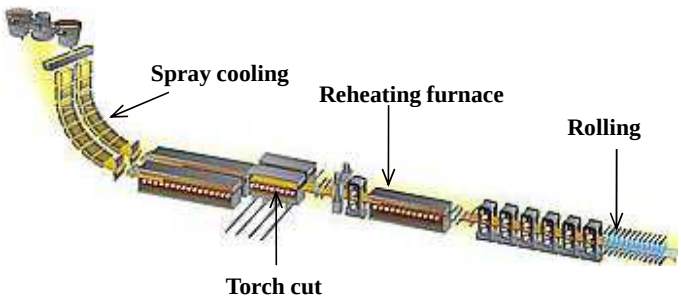

Cracks form during cooling due to:

- tensile stress

- low ductility

➢ To design temperature histories to avoid crack formation, need accurate predictive tools

➢ Models can now accurately predict temperature (CON1D) and stress histories (CON2D, Abaqus)

➢ Need tools to predict metallurgical behavior to estimate hot ductility, such as grain size, precipitate formation

Mechanism of surface crack formation with precipitate embrittlement

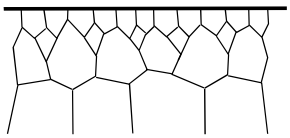

STAGE I - Normal solidification on mold wall. Surface grains are small but highly oriented.

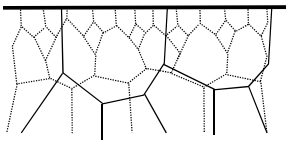

STAGE II - Surface grains "blow" locally due to high temperature (>1350°C) and strain, especially at the base of deeper oscillation marks.

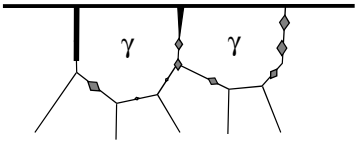

STAGE III - Nitride precipitates begin to form along the blown grain boundaries. Microcracks initiate at weak boundaries.

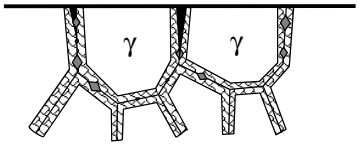

STAGE IV - Ferrite transformation begins and new precipitates form at boundaries. Existing micro-cracks grow & new ones form.

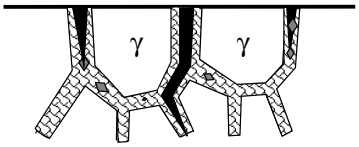

STAGE V - At the straightener, microcracks propagate and become larger cracks, primarily on top surface of the strand.

E. S. Szekeres,Proceedings of the 6th International Conference on Clean Steel, Hungary, 2002.

Hot ductility varies with temperature and grade due to precipitate formation

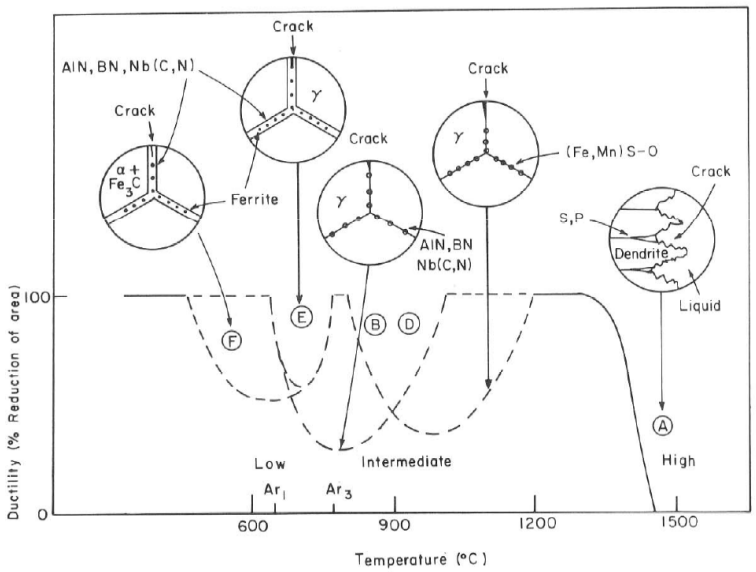

- Formation sequence of precipitates is determined by steel composition,
- γ→αphase transformation greatly accelerates the precipitation due to lower solubility and higher diffusion in ferrite

B.G. Thomas, *ISS Transactions*, 1986, pp. 7.

Project Overview

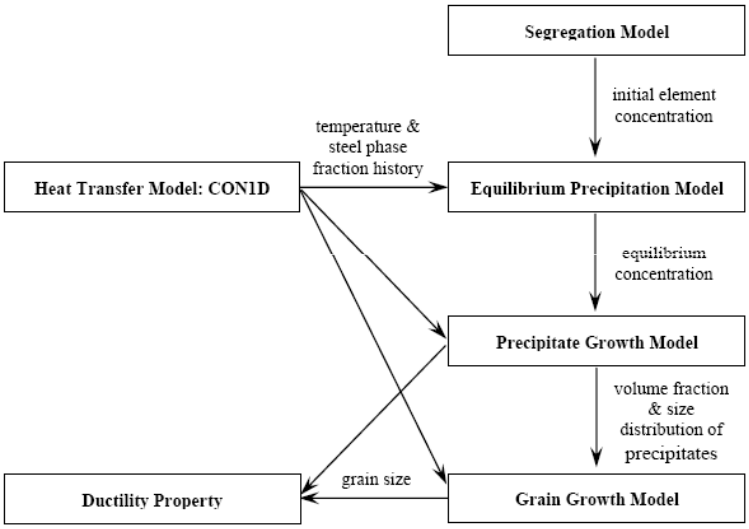

Final goal: Design casting practices to predict ductility and prevent cracks

Equilibrium precipitation model

To solve system of nonlinear equations, which include:

1. Solubility limit for each precipitate with consideration of influence on activities from Wagner interaction between elements
2. Mass balance for each element during precipitation
3. Mutual solubility

Calculate the stable precipitate phases and the dissolved mass concentrations of alloying elements in microalloyed steels for the given temperature

k. Xu, B. G. Thomas and Ron O'Malley, accepted by *Metall. Mater. Trans.* A, 2010

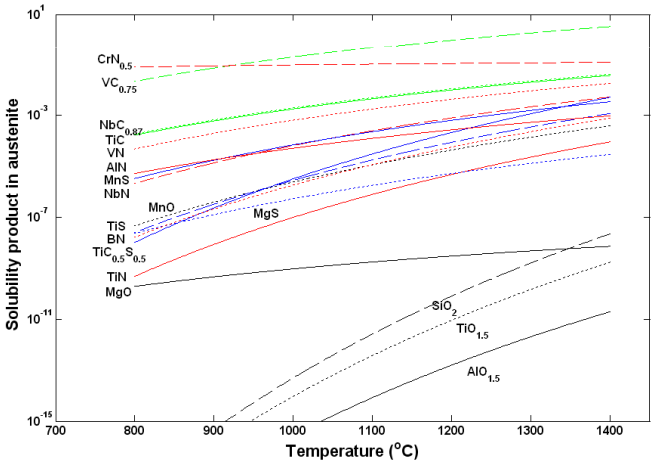

Comparison of precipitate calculations by software JMat-Pro and current model

Steel	Al	C	Cr	Mn	Mo	N	Nb	S	Si	Ti	V	O
1004 LCAK	0.040	0.025	0.025	0.141	0.007	0.006	0.002	0.0028	0.028	0.0013	0.001	0.00015
1006Nb HSLA	0.0223	0.0472	0.0354	0.9737	0.0085	0.0083	0.0123	0.0013	0.2006	0.0084	0.0027	0

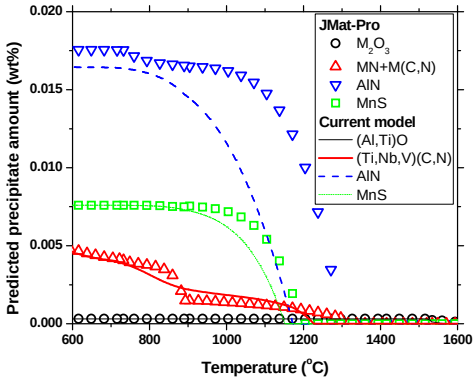

1004 LACK

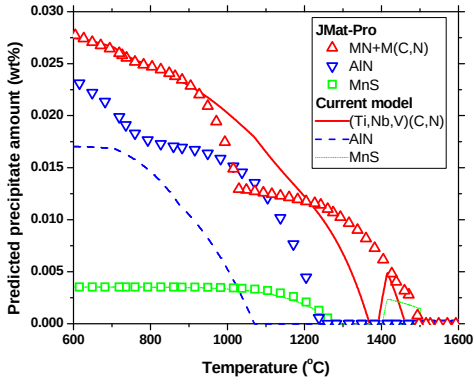

1006Nb HSLA

- **JMat-Pro predicts a TiN-rich "MN" phase at higher temperatures and a NbC-rich "M(C,N)" phase at lower temperatures, but single (Ti,Nb,V)(C,N) phase in current model**
- **For 1006Nb steel the calculated composition is $Ti_{0.48}Nb_{0.02}V_{0.00}C_{0.00}N_{0.50}$ (1304°C) and $Ti_{0.28}Nb_{0.22}V_{0.00}C_{0.23}N_{0.27}$ (804°C) for JMat-Pro, and $Ti_{0.47}Nb_{0.03}V_{0.00}C_{0.02}N_{0.48}$ (1304°C) and $Ti_{0.29}Nb_{0.21}V_{0.02}C_{0.14}N_{0.35}$ (804°C) for current model**

Different stages in precipitation

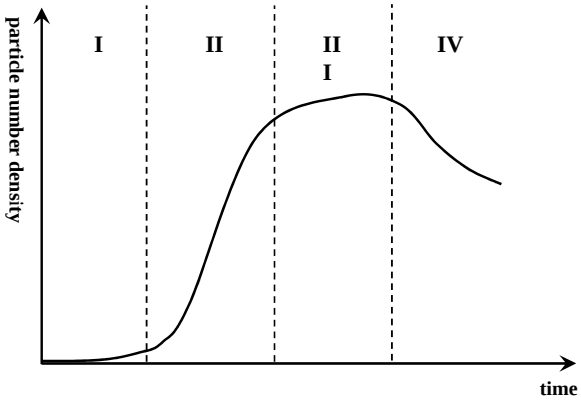

I. Induction period;
II. Steady state nucleation;
II. Decreasing nucleation rate due to decreasing supersaturation
IV. Particle coarsening

Governing equations for precipitation

1. Nucleation (W. J. Liu, *Metall. Trans. A. 1989. pp.689*)

Steady state nucleation rate $J = \frac{\rho D X_{Ti}}{a^3} \exp\left(-\frac{\Delta G^*}{KT}\right)$ $\Delta G = V(\Delta G_{chem} + \Delta G_\varepsilon) + S\xi\sigma$

For TiC_yN_{1-y} $\Delta G_{chem} = RT/(2V_P)\left[\ln\left(X_{Ti}^e / X_{Ti}^0\right) + y\ln\left(X_C^e / X_C^0\right) + (1-y)\ln\left(X_N^e / X_N^0\right)\right]$

ρ: Dislocation density, a: lattice parameter, D: diffusion coefficient, V_P: molar volume

Precipitation start time $P_s = N_c / J$ N_c: critical number of nuclei for precipitation

2. Precipitate growth (L. M. Cheng, *Metall. Mater. Trans. A, 2000, pp.1907*)

$$\frac{dr}{dt} = \frac{C_M - C_I}{C_P - C_I}\left[\frac{D}{r} + \left(\frac{D}{\pi t}\right)^{1/2}\right]$$ Gibbs-Thomson relation $C_I = C_e^\infty \exp\left(\frac{2\sigma V_P}{R_g T r}\right)$

Concentration: matrix C_M, matrix/precipitate interface C_I, precipitate C_P

➢Diffusion growth (Zener, *J. Appl. Phys.*, 1949, pp.950)

$$\bar{r}^2 - \bar{r}_0^2 = \alpha D(t - t_0)$$

➢Coarsening (Lifshitz-Slyozov-Wagner equation, 1961) $\bar{r}^3 - \bar{r}_0^3 = \frac{8\sigma D V_P C_M}{9R_g T}(t - t_0)$

Fundamental kinetic model for precipitate growth

Particle diffusion $$\frac{dn_i}{dt} = \underbrace{-\beta_i n_1 n_i}_{\text{Particle Diffusion (i→i+1)}} + \underbrace{\beta_{i-1} n_1 n_{i-1}}_{\text{Particle Diffusion (i-1→i)}} \underbrace{- \alpha_i A_i n_i}_{\text{Particle Dissolution (i→i-1)}} + \underbrace{\alpha_{i+1} A_{i+1} n_{i+1}}_{\text{Particle Dissolution (i+1→i)}} \quad (i \geq 2)$$

n_i: Number density of size i particle (#/m^3)

β_i: Diffusion rate constant of size i particle (m^3/s) $\beta_i = 4\pi D_1 r_i$

α_i: Dissolution rate per unit area of size i particle ($m^{-2}s^{-1}$) $\alpha_i = \beta_i n_{1,eq} \exp\left(2\sigma V_m / RTr_i\right) / A_i$

➢ It includes nucleation, growth/dissolution and coarsening in one single model, and no fitting parameters are introduced

➢ The particles of every size are tracked in the model, ranging from single molecule, unstable embryos, stable nuclei to very large coarsening particle

➢ The computational cost quickly becomes infeasible for realistic particle sizes

Introduction of particle-Size-Grouping (PSG) method

- The model always simulates from single molecule (~ 0.1nm) up to large coarsened particles (~100μm): particles could contain 1~10^{18} molecules
- Serious computation and memory storage issues arise with such a large size range
- Solve with PSG method: Use N_G groups (<100) of geometrically progressing size

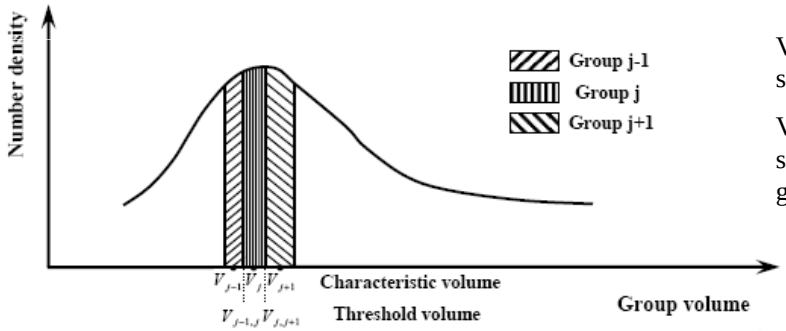

V_j: Characteristic volume of size group j particle

$V_{j,j+1}$: Threshold volume to separate group j and j+1 size group particles

$$V_{j,j+1} = \sqrt{V_j V_{j+1}}$$

Average particle volume ratio

$$R_V = V_{j+1} / V_j$$

Total number density of each size group $N_j = \sum_{V_{j,j+1} > V > V_{j-1,j}} n(V)$

Develop new PSG method for diffusion

$$\frac{dN_j}{dt} = \underbrace{\frac{m_1}{m_j}\beta_j N_1 (N_j - n_j^U)}_{\text{Diffusion inside group j}} - \underbrace{\frac{m_1}{m_j}\alpha_j A_j (N_j - n_j^L)}_{\text{Dissolution inside group j}} + \underbrace{\frac{ceil(V_{j-1,j})}{V_j}\beta_{j-1}^U N_1 n_{j-1}^U}_{\text{Diffusion group j-1→j}} + \underbrace{\frac{floor(m_{j,j+1})}{m_j}\alpha_{j+1}^L A_{j+1}^L n_{j+1}^L}_{\text{Dissolution group j+1→j}}$$

$$\underbrace{-\frac{floor(m_{j,j+1})}{m_j}\beta_j^U N_1 n_j^U}_{\text{Diffusion group j→j+1}} \underbrace{-\frac{ceil(m_{j-1,j})}{m_j}\alpha_j^L A_j^L n_j^L}_{\text{Dissolution group j→j-1}} \quad (j \geq 2)$$

n_j^L : Number density of particles in size group j, which jumps into group j-1 by dissolution after losing only one single molecule

n_j^U : Number density of particles in size group j, which jumps into group j+1 by diffusion after gaining only one single molecule

m_j and $m_{j,j+1}$ are the containing number of molecules for the characteristic volume V_j and the threshold volume $V_{j,j+1}$. Function ceil(x) calculates the smallest integer which is not less than x, and floor(x) calculates the largest integer which is not larger than x

Calculation of size-border particle threshold values

The size-border particle number densities are estimated from geometric progression of number densities for two neighboring size groups.

Average number densities $\bar{n}_j = \dfrac{N_j}{floor(m_{j,j+1}) - ceil(m_{j-1,j}) + 1}$

Common ratios $q_j^L = \left(\dfrac{\bar{n}_j}{\bar{n}_{j-1}}\right)^{\frac{1}{m_j - m_{j-1}}}$, $q_j^R = \left(\dfrac{\bar{n}_{j+1}}{\bar{n}_j}\right)^{\frac{1}{m_{j+1} - m_j}}$

Number densities at center of size group $n_j^C = \dfrac{N_j}{\sum_{k=1}^{m_j - ceil(m_{j-1,j})} (1/q_j^L)^k + 1 + \sum_{k=1}^{floor(m_{j,j+1}) - m_j} (q_j^R)^k}$

Threshold values $n_j^L = n_{j-1}^C \left(\dfrac{n_j^C}{n_{j-1}^C}\right)^{\frac{ceil(m_{j-1,j}) - m_{j-1}}{m_j - m_{j-1}}}$, $n_j^R = n_j^C \left(\dfrac{n_{j+1}^C}{n_j^C}\right)^{\frac{floor(m_{j,j+1}) - m_j}{m_{j+1} - m_j}}$

For particle growth, if $N_j \neq 0$ and $N_{j+1} = 0$ $n_j^R = n_j^L \left(\dfrac{n_j^C}{n_j^L}\right)^{\frac{floor(m_{j,j+1}) - m_j}{m_{j+1} - m_j}}$

For stability, implicit Euler scheme is applied for practical problem with iterative Gauss-Seidel method until the largest relative difference of all N_j between two iterations is smaller than 10^{-5}

Validation of test problem for diffusion

Dimensionless form $n_i^* = n_i / n_{1,eq}$ $t^* = 4\pi D_1 r_1 n_{1,eq} t$

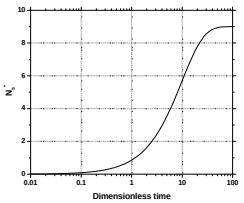

Molecules produced by an isothermal first order reaction

$$n_s^*(t^*) = n_s(t^*)/n_{1,eq} = \sum_{i=1}^{n_M} i \cdot n_i^* = 9[1 - \exp(-0.1t^*)]$$

Initial condition (t*=0): $n_i^*=0$ for $i \geq 1$ (same for N_i in PSG model)

Boundary condition: $n_M^*=0$, or $N_G^*=0$ at all t*

Exact solution: $n_M=50000$; **PSG model**: $N_G=18$ ($R_V=2$) or $N_G=13$ ($R_V=3$)

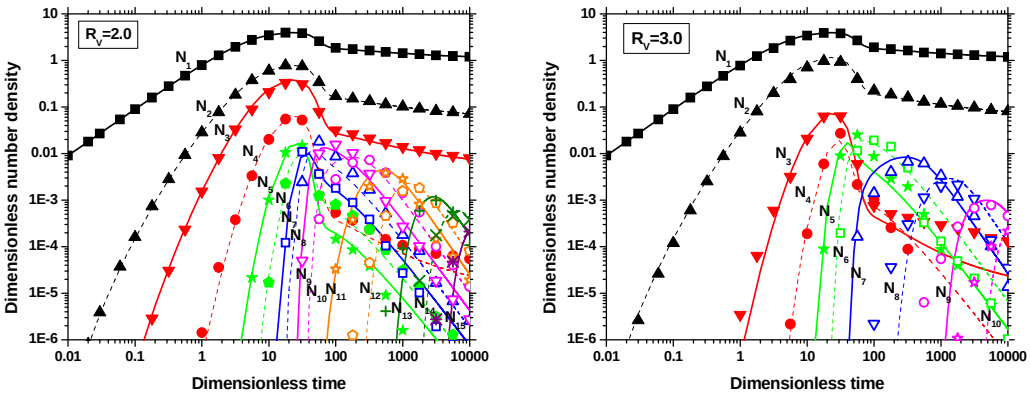

Average particle size with time

Precipitate particle (containing 23 or more molecules, size group ≥6 for PSG method R_V=2)

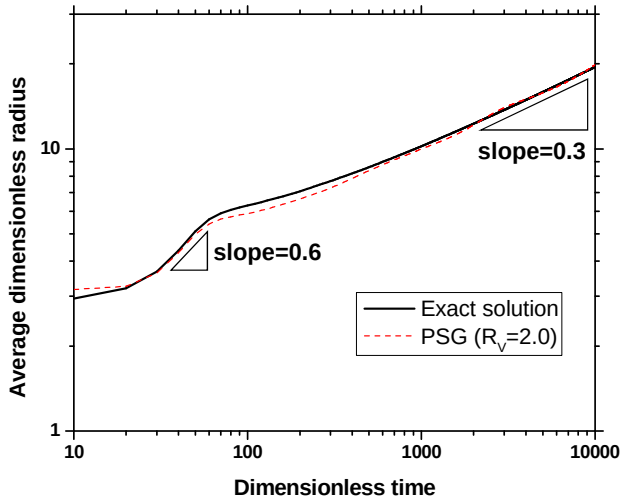

Theoretical value: slope=0.5 at growth stage, slope=0.33 for coarsening stage

Comparison of computation for test problems

	Diffusion (t*=10000)		
	Exact	**PSG (R_V=2)**	**PSG (R_V=3)**
Storage	**n_M=50000**	**N_G=18**	**N_G=13**
Computational time	**~27 hours**	**~560s**	**~390s**

* Calculation is run with Matlab on Dell OPTIPLEX GX270 with P4 3.20GHz CPU and 2GB RAM

- For constant R_V, the number of size groups in PSG method must satisfy

  $V_{N_G} = R_V^{N_G-1} > n_M \rightarrow N_G = Ceil(\log_{R_V} n_M)+1+1$ (last one for boundary group)

- The computational time is proportional to n_M or N_G for diffusion problem
- It only uses less than 60 size groups to cover particle sizes up to 100μm with constant R_V=2 for most nitrides and carbides
- Computation cost is dramatically reduced, especially for the problem with a large variety of precipitate sizes because of logarithm relation

Determination of interfacial energy

$$\sigma = \sigma_c + \sigma_{st}$$

$$\sigma_c = \frac{\Delta E_0 N_s Z_s}{N_A Z_l}(X^P - X^M)^2$$

D. Turnbull, *ASM*, 1955, pp.121.

K. C. Russell, *Adv. Colloid Interface Sci.* , 1980, pp.205.

J. H. Van Der Merwe, *J. Appl. Phys.* , 1963, pp. 117.

ΔE: heat of solution, N_s: number of atoms per unit area across the interface, Z_s: number of bonds per atom across the interface, Z_l: coordinate number of nearest neighbors within the crystal, X^P, X^M: molar concentration in precipitate and matrix (X_P=0.5>> X_M=0 for AlN)

$$\sigma_{st} = \frac{\mu c}{4\pi^2}\left\{1+\beta-(1+\beta^2)^{1/2}-\beta\ln\left[2\beta(1+\beta^2)^{1/2}-2\beta^2\right]\right\}$$

$$\frac{2}{c} = \frac{1}{a_M^e} + \frac{1}{a_P^e}, \quad \frac{2}{\mu} = \frac{1}{\mu_M} + \frac{1}{\mu_P}$$

$$\beta = 2\pi\delta\frac{\lambda_+}{\mu}, \quad \delta = \frac{2\left|a_M^e - a_P^e\right|}{a_M^e + a_P^e}, \quad \frac{1}{\lambda_+} = \frac{1-\nu_M}{\mu_M} + \frac{1-\nu_P}{\mu_P}$$

c: spacing of reference lattice, μ_M, μ_P, μ (a_M, a_P, a): shear modulus (lattice parameter) of matrix, precipitate and interface, δ: lattice misfit across the interface

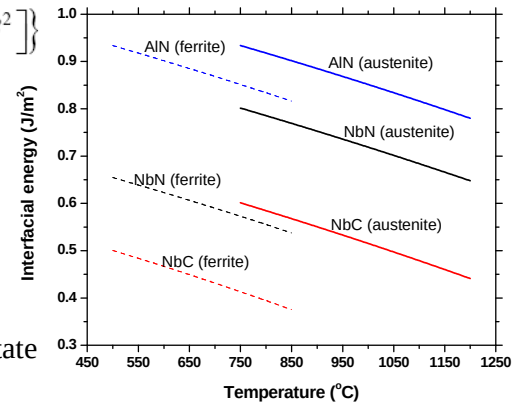

Validation cases for precipitate growth

Three steps model: 1) Heat transfer model , CON1D, gives the temperature and steel phase histories

2) For the given temperature histories, equilibrium model gives the equilibrium dissolved mass concentration of the alloying element, which is stoichiometrically insufficient to form precipitate (maximum amount of precipitate that possibly forms) at each temperature

3) Kinetic model of precipitate growth gives the precipitated fraction and size distribution of precipitatete particles for the given temperature histories

Initial only single molecules $n_s = \frac{M_0\rho_{steel}}{100A_M}N_A$, equilibrium number density $n_{1,eq} = \frac{[M]\rho_{steel}}{100A_M}N_A$

Validation cases: 1). Particle size ddistribution of NbC particles annealing at 930°C

2). Precipitated fraction of N for AlN precipitate annealing at 840°C (austenite) and 700°C (ferrite)

3). PTT diagram of Nb(C,N) precipitate annealing at 850-950°C

4). Colorado school measurements for the precipitated fraction of Nb in practical casting and reheating processes

Case 1: Validation of NbC particle size distribution

- Steel composition: 20% Cr, 25% Ni, 0.5% Nb, 0.05% C+N.
- Solution treated at 1350°C, quenching and aged at 930°C for 1800s with no deformation prior to ageing, $D_{Nb}(m^2/s)=0.83\times10^{-4}\exp(-266500/RT)$
- Equilibrium calculation (0.05wt% assumed to pure C): NbC forms at 1310°C, [C]=0.0052wt% at 930°C, $\sigma=0.54J/m^2$, truncating radius 0.5nm (carbon extraction)

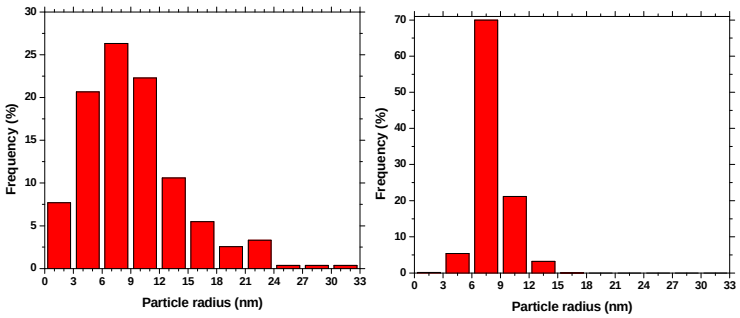

Experiment Simulation

Measured particle size distribution is always wider than simulation due to existence of grain boundaries. The result is worsen by alloying nitrogen and possible Cr carbonitride formation .

A. R. Jones, *J. Mater. Sci.*, 1976, pp.1600

Case 2: Validation of AlN precipitated fraction

- Steel composition: 0.09% C, 0.20% Si, 0.36% Mn, 0.051% Al, 0.0073% N. The
- Solution treated at 1300°C for 2 hours, cooled to the test temperature and held. $D_{Al}(m^2/s)=2.51\times10^{-4}\exp(-253400/RT)$ in austenite and $D_{Al}(m^2/s)=0.3\times10^{-2}\exp(-234500/RT)$ in ferrite. Measurements are normalized with equilibrium calculation.
- Equilibrium calculation: AlN forms at 1236°C, $[N]=2.2\times10^{-4}$wt% and $\sigma=0.908J/m^2$ at 840°C, $[N]=3.1\times10^{-6}$wt% and $\sigma=0.997J/m^2$ at 700°C

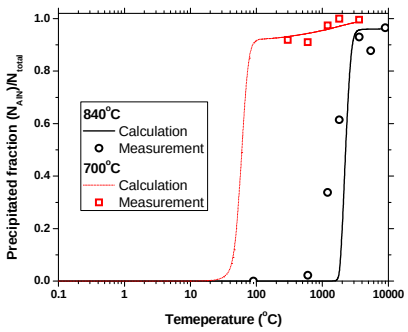

- Truncating radius 2nm (Beeghly), since we track every size (smaller than stable nuclei) and experiments have resolution limit
- Precipitation in ferrite is greatly accelerated, due to much lower solubility limit and higher diffusion rate even at a lower temperature

F. Vodopivec, *J. Iron Steel Inst.*, 1973, pp.664

Case 3: Equilibrium calculation for C-Mn-Nb steel

Steel composition: (S. H. Park, Metall. Trans. A, 1992, pp. 1641)

Steel	C	Mn	Si	S	P	Nb	Al	N
C-Mn-Nb	0.067	1.23	0.20	0.008	0.008	0.040	0.020	0.006

Solution treated at 1150°C for 30 min, cooled down to test temperature, held for 1 min to stabilize and 5% deformation is executed. The stress decreases with time in stress relaxation testing

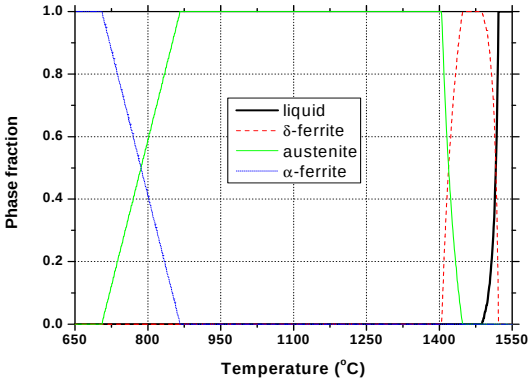

Steel phase

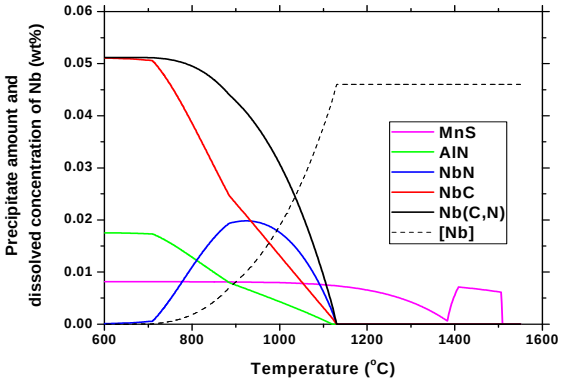

Precipitate phases

Case 3: Calculation of precipitation start and finish time

Truncating radius 0.8nm,
Effective interfacial energy σ_e= 0.475σ, $\sigma_{Nb(C,N)} = x^e_{NbN}\sigma_{NbN} + x^e_{NbC}\sigma_{NbC}$
(to account for 5% deformation)

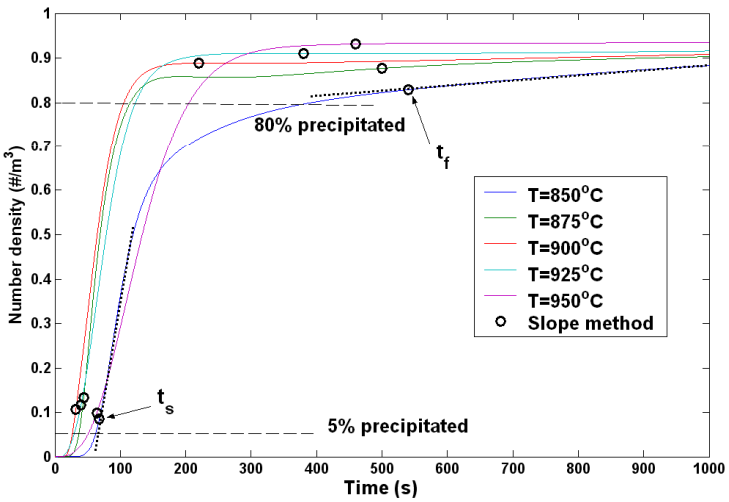

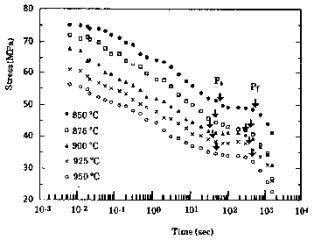

S. H. Park, *Metall. Trans. A*, 1992, pp. 1641

Slope method: corresponds with experimental technique (slope transition points on the stress-time plot)

Case 3: Comparison of precipitation start and finish time

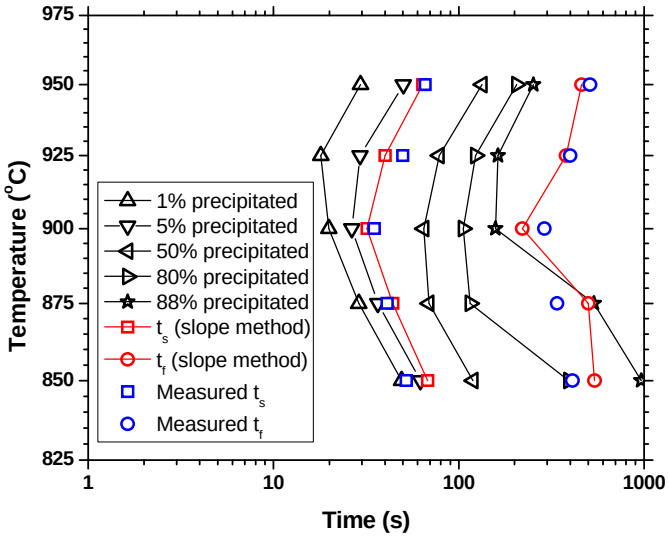

- "C" shape is caused by two competing mechanisms in precipitation: high supersaturation in low temperature and high diffusion rate in high temperature

Case 3: Particle size distribution evolution

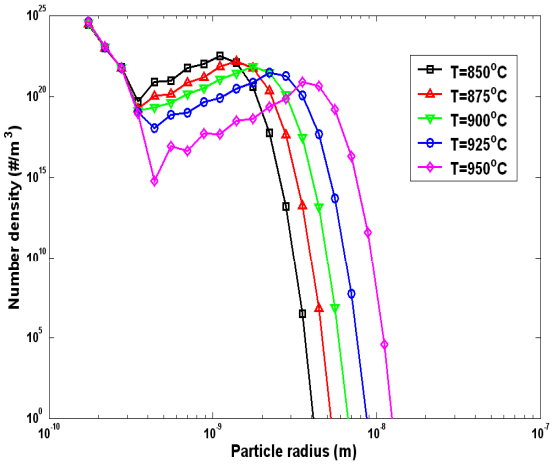

t=1000s

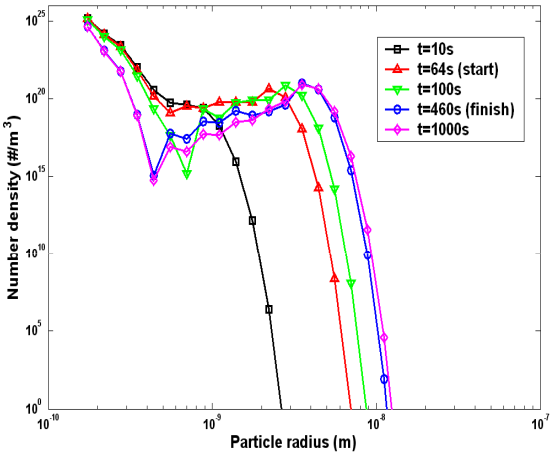

T=950°C

- Finer particle size distribution is observed for lower temperature due to larger supersaturation and lower diffusion rate
- The particle size increases slowly in coarsening stage

Case 3: Influence of diffusion rate on precipitation

t=1000s

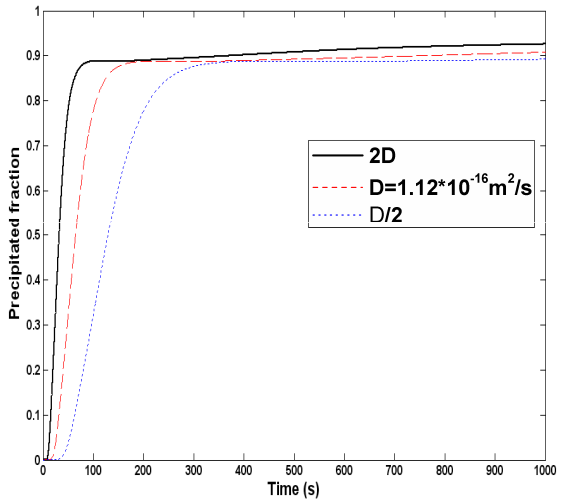

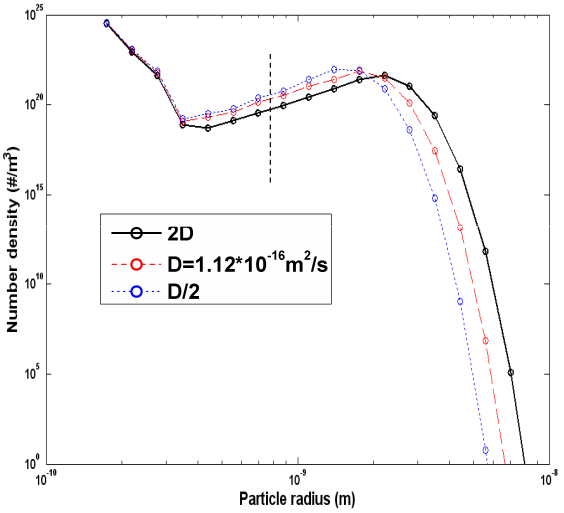

➢ **Precipitation start time, finish time and mean particle size are all proportional to diffusion rate**

Case 3: Influence of supersaturation on precipitation

t=1000s

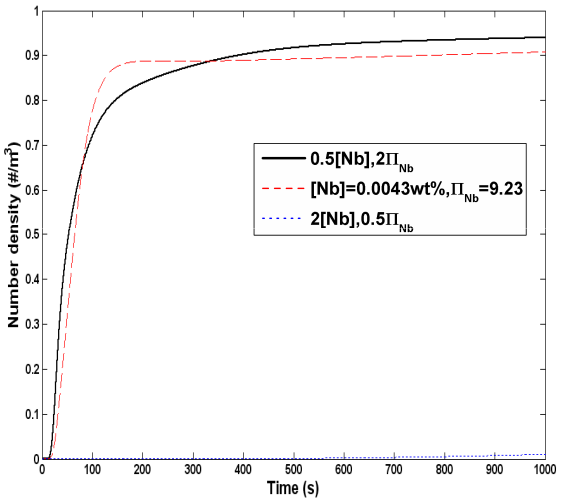

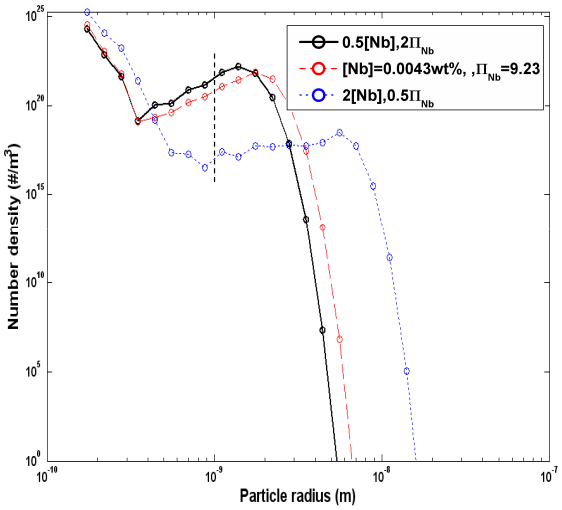

➢ **Higher supersaturation increases the precipitation process and cause the finer particle size distribution (higher nucleation rate)**

Case 3: Influence of interfacial energy on precipitation

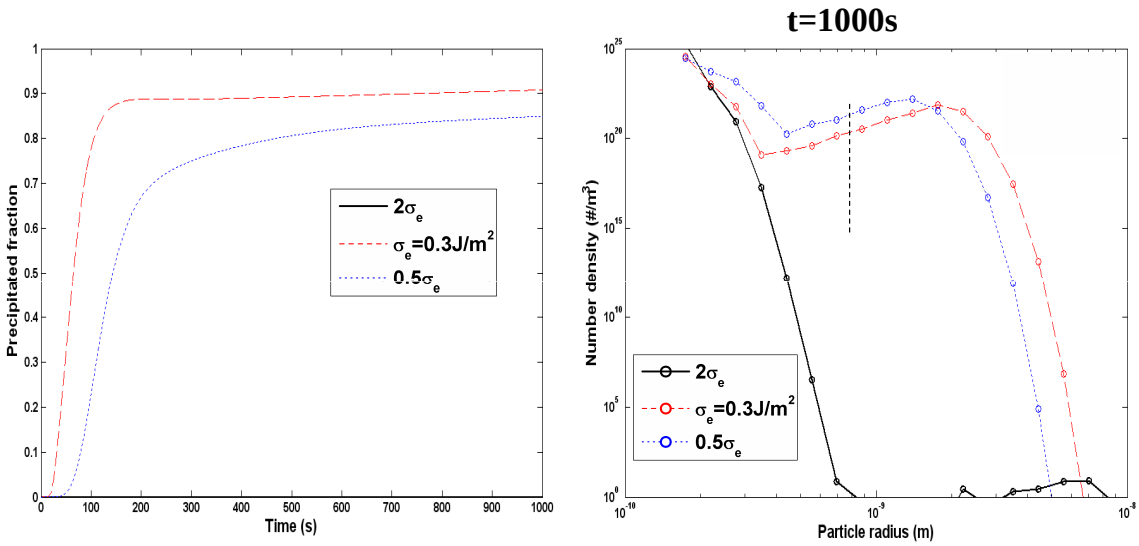

- **Smaller interfacial energy causes finer particle size distribution and less larger stable particles formed due to smaller capillary effect.**
- **Larger interfacial energy brings higher precipitation barrier due to much larger dissociation rate (close to no deformation case)**

Case 4: Colorado school experiments

- The effects of microalloy precipitation and (tunnel furnace) dissolution during direct strip production are explored relative to the position within the slab and alloy content.
- Niobium solute and precipitation fractions are quantified using electrochemical extraction and inductively coupled plasma atomic emission spectrometry (ICP-AES).
- The greatest amount of alloy precipitation occurs at the slab surface of the thin slab. The extent of precipitation appears greatest for high niobium steel, where dissolution subsequently occurs during reheating in the tunnel furnace. The columnar region represents the bulk of the slab volume and exhibits the lowest precipitated amount.

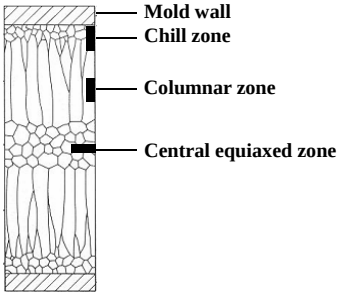

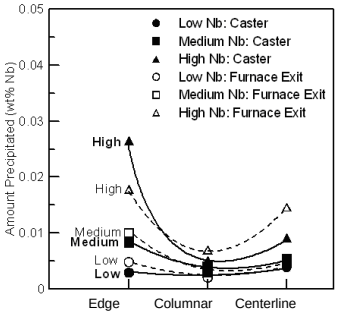

Myra S. Dyer, Microalloy Precipitation in Hot Charged Slabs, 2010 AIST.

Case 4: Temperature and steel phase model

CON1D Program: Solve the transient heat conduction in the mold and spray regions of continuous steel slab casters using finite difference method

Example: thin slab casting of low-carbon High Nb steel

Steel	C	Mn	Si	Al	Nb	P	S	N
High Nb	0.031	1.039	0.194	0.031	0.046	0.012	0.003	0.006

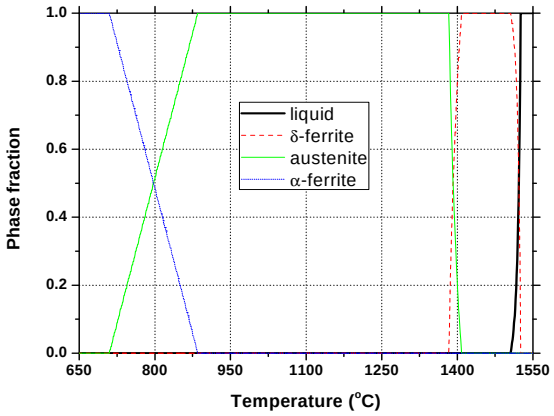

Slab size: 50mm thick, 1500mm wide
Mold exit: 0.8m below meniscus
Pouring Temperature: 1553°C
Casting speeds: 5m/min
Spray zone: 0.8-11.25m (estimated)

Liquidus temperature: 1525.70°C
Solidus temperature: 1506.13°C

Case 4: Equilibrium calculation for High Nb steel

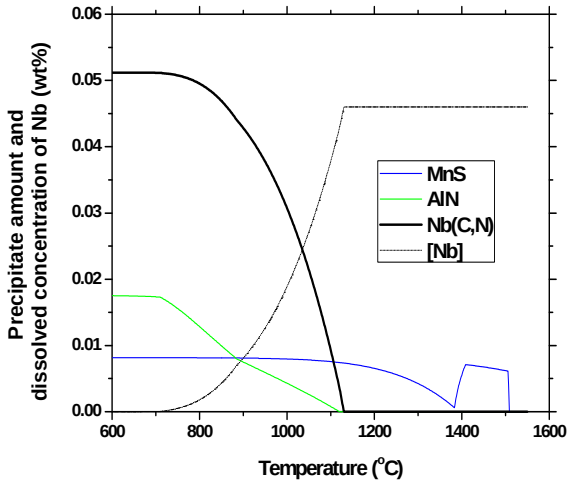

Precipitate phases

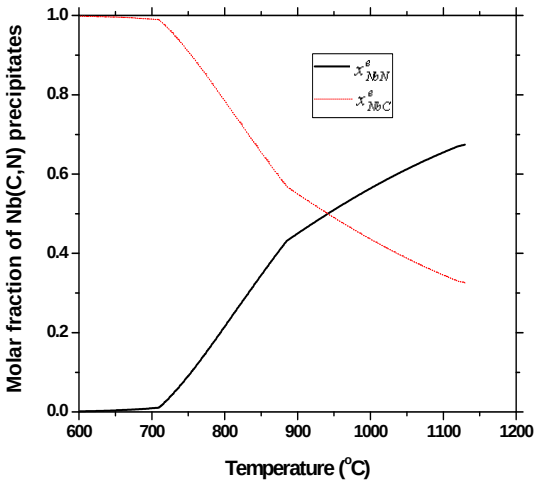

Molar fraction of Nb(C,N)

Case 4: Temperature prediction (casting)

- **casting→air cooling→quenching case**

Sample is air cooled for 6m after the end of casting, then water quenching with heat transfer coefficient h=2000W/(m^{2}K), $D=f_\gamma D_\gamma+f_\alpha D_\alpha$

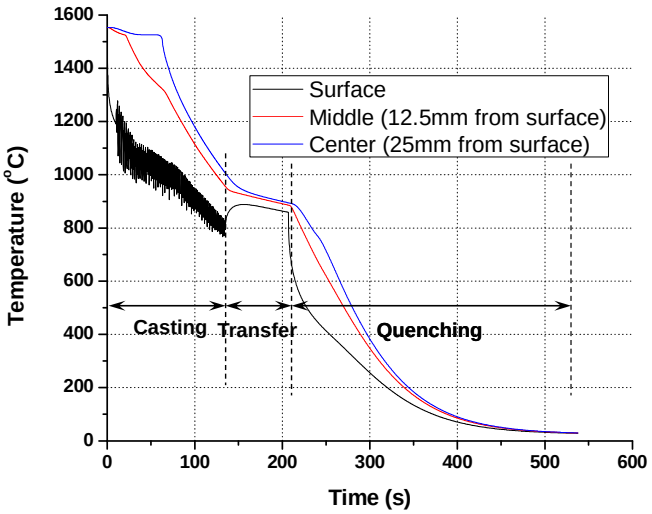

$$D_\gamma(m^2/s) = 0.83\times10^{-4}\exp(-266490/RT)$$
$$D_\alpha(m^2/s) = 50.2\times10^{-4}\exp(-251970/RT)$$
$$\bar{\sigma}_{Nb(C,N)} = 0.5J/m^2$$

Case 4: Comparison of precipitated fraction of Nb (casting)

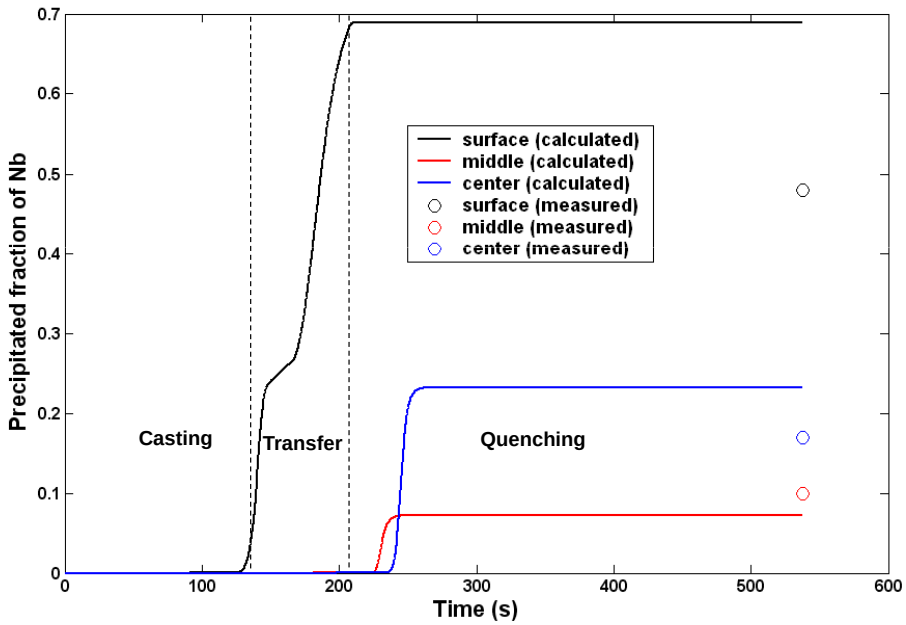

Myra S. Dyer, Microalloy Precipitation in Hot Charged Slabs, 2010 AIST.

Case 4: Particle size distribution (casting)

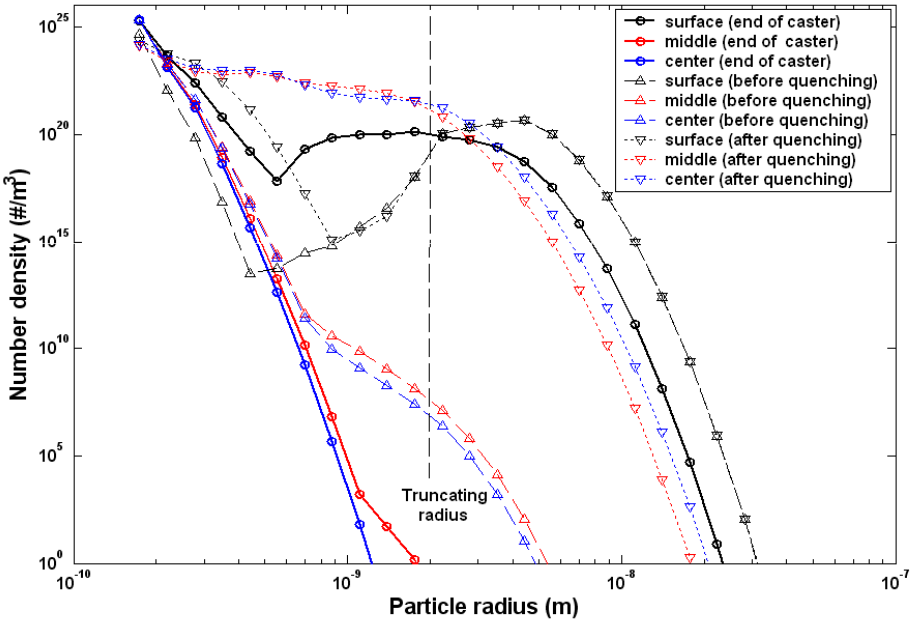

Case 4: Temperature prediction (casting+reheating)

- **casting→air cooling→reheating→quenching case**

Sample is air cooled for 15m after the end of casting, then enters the 75m long reheating furnace with reference temperature 1050°C (air heated), finally water quenched with heat transfer coefficient h=2000W/(m²K), $D=f_\gamma D_\gamma+f_\alpha D_\alpha$

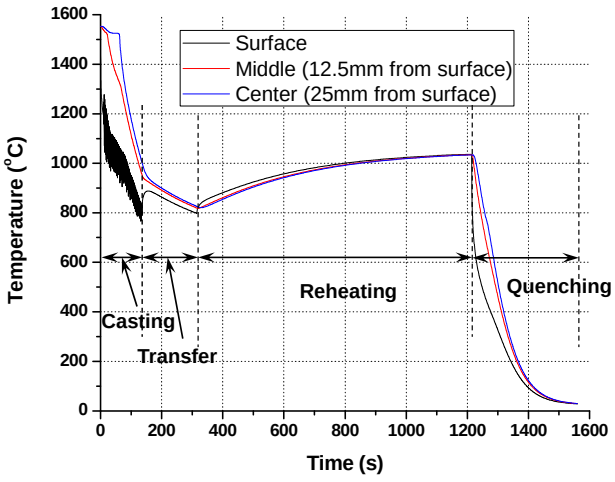

Case 4: Comparison of precipitated fraction of Nb (casting+reheating)

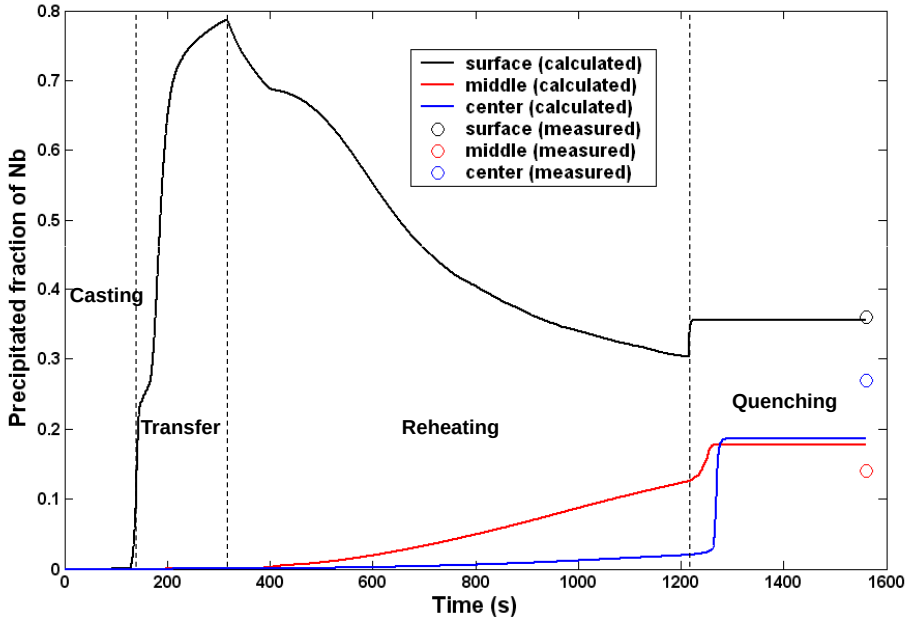

Myra S. Dyer, Microalloy Precipitation in Hot Charged Slabs, 2010 AIST.

Case 4: Particle size distribution (casting+reheating)

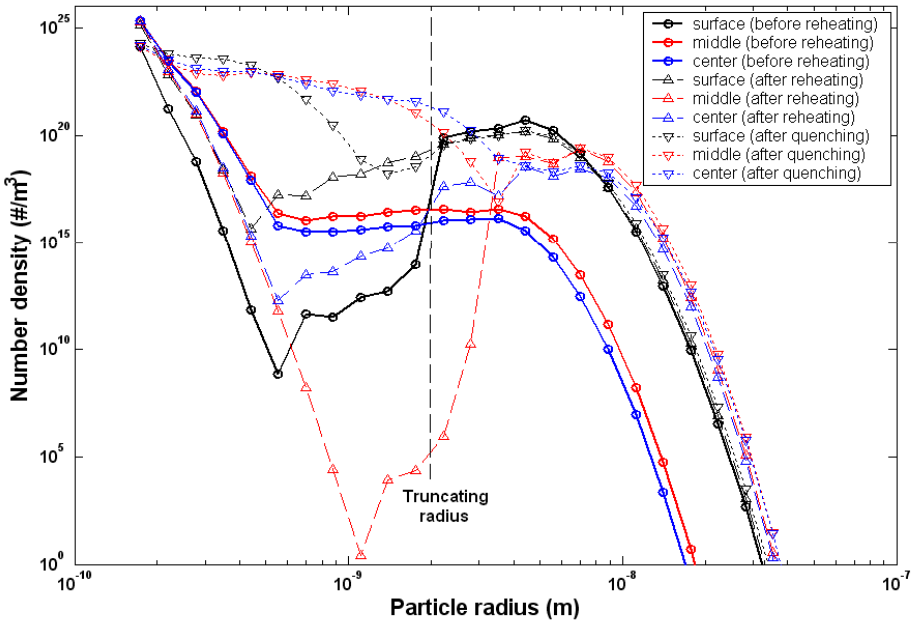

Case 4: Kinetic calculation of NbN/NbC molar fractions on the slab surface

- The molar fractions of newly formed or dissolved precipitates at each time step is determined by the equilibrium molar fractions at this time step
- Add the product of the newly formed precipitated fraction and the equilibrium molar fractions together, and the final value is divided by total precipitated fraction to get the non-equilibrium molar fractions with kinetic consideration
- The molar fraction at the beginning is not trustable since numerical error is maybe introduced because of too small precipitated fraction

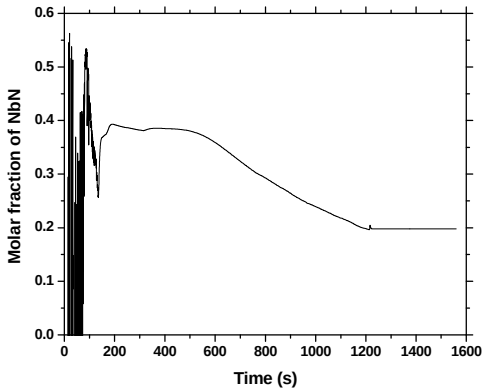

$$x_{NbN} = \frac{\sum_{i=1}^{n} (\Delta f_P)_i \cdot (x^e_{NbN})_i}{(f_P)_n}, \quad x_{NbC} = 1 - x_{NbN}$$

- The molar fraction is not the same as ~0 at room temperature in equilibrium model, because the kinetics at low temperature is too small
- Now we compute amounts of NbN/NbC under kinetic consideration

$$w_{NbN} = f_P \cdot x_{NbN} \cdot Nb_0 \cdot A_{NbN} / A_{Nb}$$

$$f_{NbN} = \rho_{steel} w_{NbN} / (100 \rho_{NbN})$$

Count pinning effects from both NbN and NbC

Case 4: Austenite grain growth model

Grain growth in austenite under the presence of precipitates

$$\frac{d\bar{D}}{dt} = M_0^* \exp\left(-\frac{Q_{app}}{RT}\right)\left[\frac{1}{\bar{D}} - \frac{1}{k}\frac{f}{r}\right]^{(1/n-1)}$$

M_0*: Kinetic constant that represents grain boundary mobility (m^2/s)

Q_{app}: Apparent activation energy for grain growth (J/mol)

n: Exponent to measure resistance to grain boundary motion (n=0.5 for pure material)

f and r: the volume fraction and radius of precipitates

k: Zener coefficient related to pinning efficiency of the precipitates (k=4/3)

The maximum grain diameter in the presence of precipitates is defines as $\bar{D}_{Lim} = kr / f$

Calculation begins from the temperature of totally austenite structure, the initial austenite grain size is assumed to be with the order of the primary dendrite arm spacing (PDAS)

$$\lambda_1 = K (C_R)^m (C_0)^n$$

I. Andersen and Ø Grong, *Acta Metall. Mater.*, 1995.

M. E. Bealy and B. G. Thomas, *Metall. Mater. Trans. B*, 1996.

Case 4: Grain growth calculation on the slab surface

Fully austenite temperature 1382.7°C, cooling rate estimated by CON1D is 126.5°C/s, the initial grain size is 247.5μm

Instead of Zener expression for uniformly distributed particles $\bar{D}_{Lim} = 4\bar{r}/3f$, the maximum grain diameter for a size distribution is determined as

$$\bar{D}_{Lim} = 4/\left(3*\sum_j (f_j / r_j)\right)$$

The summation covers the particle with radius larger than truncating value, and the grain growth will stop when $\bar{D}_{Lim}$ decreases to be smaller than the calculated grain size $\bar{D}$

$M_0^*=4\times10^{-3}m^2/s$, n=0.5,
$Q_{app}=167686+40562(wt\%C_p)$
$wt\%C_p=wt\%C-0.14wt\%Si+0.04wt\%Mn$

J. Reiter, C. Bernhard and H. Presslinger, MS&T 2006, Cincinnati, USA.

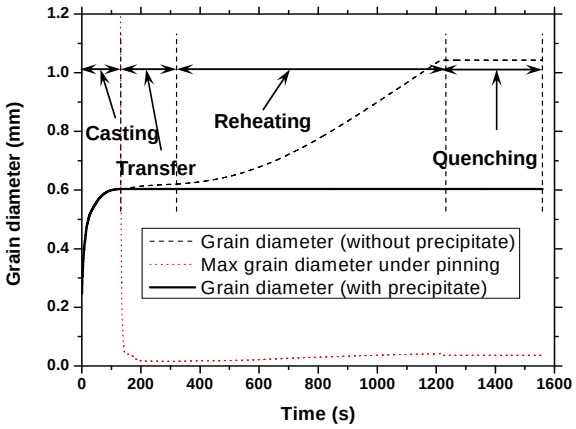

Observed multi-phase precipitates in steels

There is always more than one type of precipitate existing in steels. In fact, the previously formed precipitates could be the nucleation and growth sites of the newly formed precipitates particles.

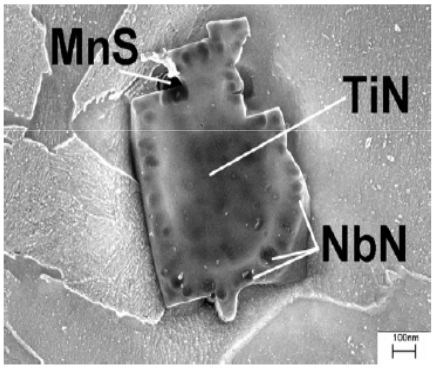

Complex precipitates with TiN core

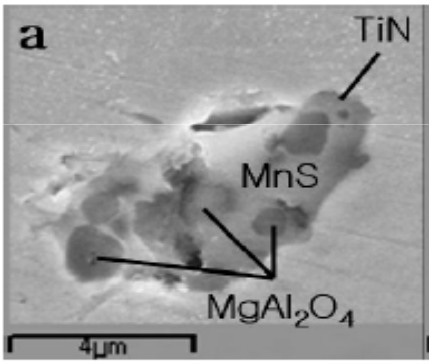

Complex precipitates with oxide core

V. Ludlow et al, Precipitation of nitrides and carbides during solidification and cooling, unpublished work.

S. C. Park, *ISIJ Int.*, 2004, pp. 1016.

Multi-phase precipitate modeling

Exact solution $$\frac{dn_i}{dt} = -\sum_{s=1}^{n_p} \beta_i^s n_1^s n_i + \sum_{s=1}^{n_p} \beta_{i-1}^s n_1^s n_{i-1} - \sum_{s=1}^{n_p} \frac{\alpha_i^s p_i^s}{\sum_{s=1}^{n_p} \alpha_i^s p_i^s} \alpha_i^s A_i n_i + \sum_{s=1}^{n_p} \frac{\alpha_{i+1}^s p_{i+1}^s}{\sum_{s=1}^{n_p} \alpha_{i+1}^s p_{i+1}^s} \alpha_{i+1}^s A_{i+1} n_{i+1}$$

- Run equilibrium calculation for all possible precipitates, $s=1, 2,\ldots, n_p$. P_i^s is the average molar fraction of precipitate type s in size i particles.
- For each size group determine: the molar fractions of each precipitate type and the number density of the variable-composition particles.
- Free molecules from all types of precipitates will have influence on the diffusion growth. The effect is similar with the increase of supersaturation.
- Composition of releasing molecule from particles is determined by the product of dissociation rate and molar fraction of each precipitate type
- The same ideas is applied to PSG method. The mass balance of each precipitate is verified for both exact solution and PSG method.
- Better accuracy and implicit scheme for multi-precipitate PSG method are still in progress, especially the calculation of precipitate molar fractions.

Conclusions

1. **A systematic method is established for calculating the single precipitate growth in microalloyed steels for practical processing, which includes a equilibrium model to give equilibrium dissolved concentration, and a kinetic model to give particle size distribution base on equilibrium calculation**
2. **The implicit PSG method makes the computation of particle growth efficiently. It includes nucleation, growth/dissolution and coarsening in one single model, and all parameters are fundamental based with physical significance. The good matches are found between the PSG method and exact solution for the test problem.**
3. **The calculated results match well with the experimentally measured particle size distribution of NbC and precipitated fraction of AlN. The precipitation in ferrite is proved to be greatly accelerated due to much lower solubility and higher diffusion rate.**
4. **The "C" curve of the PTT diagram is calculated as the experimental observation. The deformation is proved to greatly decrease interfacial energy and accelerate the precipitation process.**

Conclusions (CSM)

1. **The coupled model is applied to the high-Nb hot charged slab in continuous casting and reheating. The calculated results of precipitated fraction of Nb on the surface, middle and center region of the slab all match reasonably with measurements.**
2. **For the slab surface, the precipitation starts at the end of water spray cooling zone. Some precipitates are proved to dissolve in the reheating furnace, and quenching has minor influence due to locally high cooling rate on the surface.**
3. **For the inside of the slab, the precipitation starts at the reheating furnace. The quenching has important influence since the cooling inside the slab is slower for thick slab (50mm).**
4. **The grain growth stops at the end of casting due to pinning effect of Nb(C,N). Much finer grain diameter 0.6mm is found with pinning effect of precipitate (~1.0mm without precipitate)**

Future work

1. The multi-phase precipitate growth model is being developed, and needs to be verified with experiments and applied in practical steel processes
2. The precipitate model will be coupled with grain growth model to predict the grain size, especially for the larger grains under oscillation marks and near slab corner where high temperature is expected and transverse cracks are mostly possible to occur
3. The precipitate model will be coupled with segregation model to predict the precipitation on the grain boundaries, where larger precipitate particles are observed

Acknowledgements

- Continuous Casting Consortium Members (ABB, Arcelor-Mittal, Baosteel, Corus, LWB Refractories, Nucor Steel, Nippon Steel, Postech, Posco, ANSYS-Fluent)

- Colorado School of Mines, M.S. Dyer, J.G. Speer, D. K. Matlock

- Prof. B. G. Thomas